JACS
JOURNAL OF THE AMERICAN CHEMICAL SOCIETY

pubs.acs.org/JACS

Article

Hydration of a 2D Supramolecular Assembly: Bitartrate on Cu(110)

Chenfang Lin, George R. Darling, Matthew Forster, Fiona McBride, Alan Massey, and Andrew Hodgson*

Cite This: J. Am. Chem. Soc. 2020, 142, 13814−13822

Read Online

ACCESS | Metrics & More | Article Recommendations | Supporting Information

ABSTRACT: Hydration layers play a key role in many technical and biological systems, but our understanding of these structures remains very limited. Here, we investigate the molecular processes driving hydration of a chiral metal−organic surface, bitartrate on Cu(110), which consists of hydrogen-bonded bitartrate rows separated by exposed Cu. Initially water decorates the metal channels, hydrogen bonding to the exposed O ligands that bind bitartrate to Cu, but does not wet the bitartrate rows. At higher temperature, water inserts into the structure, breaks the existing intermolecular hydrogen bonds, and changes the adsorption site and footprint. Calculations show this process is driven by the creation of stable adsorption sites between the carboxylate ligands, to allow hydration of O−Cu ligands within the interior of the structure. This work suggests that hydration of polar metal−adsorbate ligands will be a dominant factor in many systems during surface hydration or self-assembly from solution.

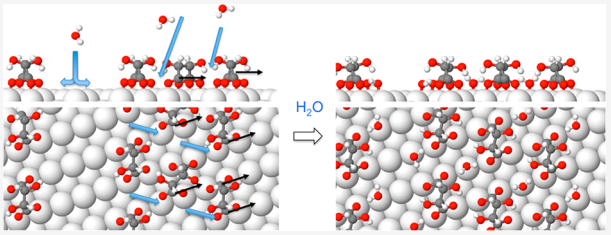

INTRODUCTION

Solvents play an important role in many chemical reactions, as they stabilize reactants, products, and intermediates differently and so alter the reaction rate and chemical selectivity, but our knowledge of their role in heterogeneous processes is remarkably limited.[1] In particular, water is becoming increasingly important as a "green" solvent to reduce waste, but its role often extends beyond the simple delivery of species to a reaction site, with hydration playing a key role in the formation of solvent−adsorbate complexes that can direct surface chemistry.[2,3] Although techniques to determine chemical identity and adsorbate structure are well developed at solid interfaces, far less is known about the local solvent environment at functional interfaces.[4] In particular, although X-ray and spectroscopic probes may provide evidence for global changes in surface hydration,[5−11] detailed molecular scale information is sparse. As a result, despite the key role that water plays in many systems,[12] insight into its molecular behavior relies largely on molecular dynamics simulations, with little experimental data to test the detail intrinsic to these models. Understanding the mechanisms by which water restructures or solvates surface species remains a significant challenge.[13,14]

Functionalized surfaces used in technical applications are typically characterized by the combination of strong surface−adsorbate bonds that bind an adsorbate to the solid surface and weaker lateral interactions that arrange the adsorbate and reactants into a particular structure or pattern on the surface. For example, hydrogen bonding can be used to assemble well-defined 2D supramolecular surface structures to chemically modify or pattern a surface to create a particular structure or function. This approach allows us to modify catalytically active surfaces to make them specific to particular adsorbates, or binding geometries, so altering the products formed. An example of this is heterogeneous chiral catalysis, where adsorption of a chiral modifier makes the surface specific to one particular enantiomer, not the other.[15] Because weak, intermolecular hydrogen bonds often play a key role in both assembly of the surface modifier and formation of a surface reaction complex, an understanding of how polar solvents, such as water, modify and hydrate surface structures is important to allow the rational design of new functionalized materials.

One approach to explore surface solvation at the molecular level is to use scanning probe microscopy to examine the initial hydration of simple surface adsorbates, which provides an insight into the detailed mechanisms involved in surface hydration. STM has been used to examine the 2D solvation shell formed around several small adsorbates,[16−20] but less is known about the way extended layers are solvated by water,[4,21,22] and imaging has yet to reveal how hydration proceeds for more complex, nonplanar adsorbates. In this study, we investigate the hydration of a 2D supramolecular structure, formed by adsorbing tartaric acid onto a metal surface. Tartaric acid is used as a chiral modifier during enantioselective catalysis and deprotonates to form an extended 2D chiral bitartrate structure on Cu(110).[23] The bitartrate is strongly bound to Cu by two bidentate carboxylate

Received: April 30, 2020
Published: July 21, 2020

https://dx.doi.org/10.1021/jacs.0c04747
J. Am. Chem. Soc. 2020, 142, 13814−13822

ligands and ordered into linear structures by weak intermolecular hydrogen bonds, with a bare metal channel separating neighboring bitartrate rows.[24] We show that water initially decorates the metal channels, forming strong hydrogen bonds to the polar O ligands exposed along the edge of the bitartrate rows. Further adsorption forms water clusters along the exposed metal channels, but does not wet the bitartrate rows, which appear hydrophobic, despite the available OH group. At higher temperature, water inserts into the bitartrate rows and breaks the hydrogen bonds that stabilize the supramolecular structure, changes the molecular adsorption site and footprint, and destroys the original chiral structure. DFT calculations show this process is driven by the creation of stable water binding sites between the polar carboxylate ligands, which allows hydration of O ligands within the interior of the supramolecular structure. Because many important systems rely on highly polar ligands to stabilize surface adsorbates, we expect that hydration of the metal−ligand sites will be of general importance in understanding how surface−adsorbate systems respond to the presence of water.

RESULTS AND DISCUSSION

Tartaric acid deprotonates the carboxylate groups at ∼400 K on Cu(110), to form an ordered chiral bitartrate phase whose behavior has been investigated in detail.[23−28] Bitartrate binds to Cu via the carboxylate O atoms to form bidentate ligands that bridge across adjacent close-packed Cu rows,[23,27] as shown in Figure 1. Under the usual experimental conditions, the bitartrate assembles into extended trimer chains, separated by a channel of bare Cu, to form the 2D chiral structure shown in Figure 1a,b. By recording STM images of low coverage regions, where aggregation into extended 2D structures is inhibited by the finite diffusion length, we are also able to identify isolated bitartrate trimers on the Cu(110) terraces, as shown in Figure 1c. The appearance of isolated trimers, in preference to individual bitartrate molecules, indicates that the trimer is the thermodynamically stable unit, consistent with DFT structure calculations that find the trimer is held together by intermolecular H-bonds, with weak dispersion and through-surface interactions assembling the trimers into rows to form the 2D structure.[24]

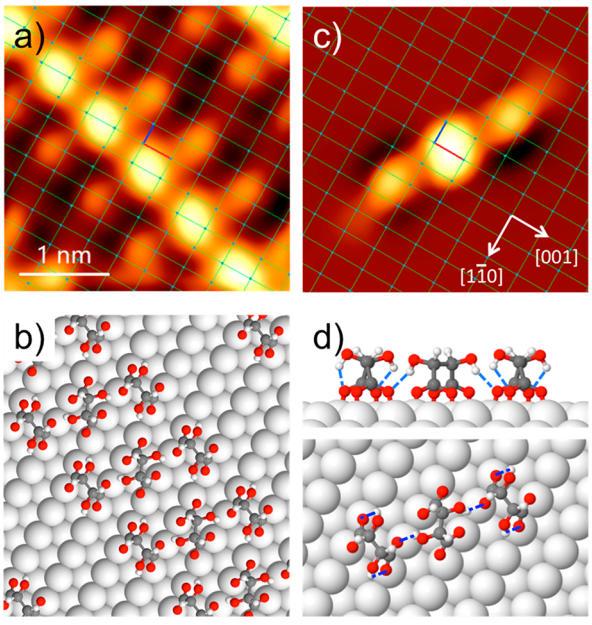

Figure 1. STM images showing (*R*,*R*) bitartrate adsorbed on Cu(110). (a) STM image showing details of the extended 2D chiral (9 0,1 2) bitartrate structure, with the surface Cu atoms indicated by the rectangular net. (b) Calculated structure for bitartrate on Cu(110). (c) STM showing an isolated $R_{ec}O_bR_{ec}$ bitartrate trimer formed at low coverage and (d) its structure, with the hydrogen bonds indicated by dashed blue lines. Images recorded at 80 K, −0.4 V, 100 pA and −0.51 V, 66 pA, respectively.

Both the isolated bitartrate trimer and the extended chain structure appear similar in STM, with the central molecule having a higher contrast than its two neighbors. Comparison of STM images with electronic structure calculations[24] shows that the trimer has a hydrogen-bonded structure in which the central bitartrate bonds to the surface with an oblique (O_b) footprint, while the two outer molecules adopt a rectangular (R_{ec}) footprint, bonded directly across neighboring Cu rows as shown in Figure 1b,d. Whereas the outer molecules are stabilized in the R_{ec} footprint by intramolecular hydrogen bonds between OH and its adjacent O ligand,[27] these hydrogen bonds are broken in the central molecule, which instead adopts an oblique footprint to allow OH to hydrogen bond to the neighboring molecules.[24] Distorting an isolated bitartrate into the O_b footprint is unfavorable, but is repaid by the formation of strong intermolecular hydrogen bonds in the $R_{ec}O_bR_{ec}$ trimer. Strain in the metal surface, caused by bonding to carboxylate,[26] prevents the bitartrate rows stacking next to each other and stabilizes the open structure (Figure 1a). Despite the high binding energy of bitartrate to Cu, the reliance on hydrogen bonds to stabilize the superstructure suggests this phase may be sensitive to the presence of water that disrupts its hydrogen bonding. Moreover, the contrast of bitartrate in STM images is sensitive to changes in its local configuration, which provides a way to explore the effect of coadsorbed water on the bitartrate structure during hydration, even when the water itself may not be directly visible by STM.

The effect of exposing a bitartrate island to water at low temperature is shown in Figure 2. Depositing a small amount of water results in the appearance of water pentamer chains on the Cu(110) terraces,[29] nucleated from the bitartrate island edges. The bitartrate islands themselves remain intact (Figure 2b), but water clusters appear as bright features at the edge of the islands and along the Cu channels between the trimer rows. These bright clusters show no particular structure and often appear diffuse, which indicates they are amorphous. At higher resolution, the Cu channels also show low contrast zigzag structures and mobile features (Figure 2c) that are easily displaced by the STM tip. The mobile features reduce as the coverage is increased, Figure 2d, with faint zigzag features apparent in parts of the Cu channel, alongside larger water clusters. The bitartrate itself appears unchanged by water adsorption and is shown superimposed on the STM image in Figure 2e. The features caused by water adsorption remain confined to the Cu channels, rather than restructuring or decorating the top of the bitartrate rows, and are attributed to weakly bound or low coordinate water that can easily be displaced within the Cu channel by the STM tip. Increasing the coverage further results in the water clusters growing larger and more numerous until they obscure the outer bitartrate molecules from view to leave only the central bitartrate rows visible between the clusters (see, for example, Figures 3g and S1 for further details). The overall behavior at low temperature is that the Cu channels act as hydrophilic sites and the

https://dx.doi.org/10.1021/jacs.0c04747
J. Am. Chem. Soc. 2020, 142, 13814−13822

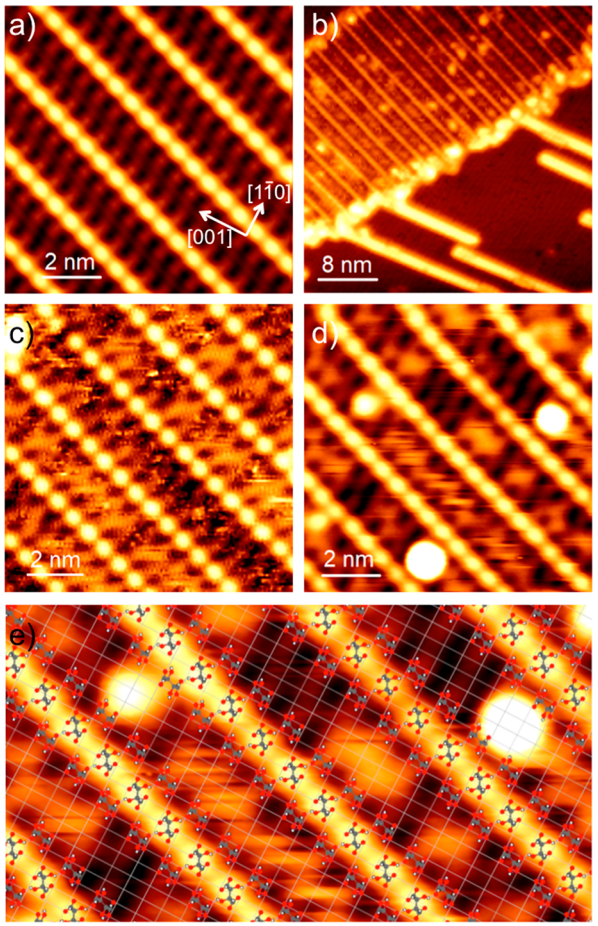

Figure 2. STM images comparing a bitartrate surface (a) before and (b–d) after water adsorption at 80 K. (b) Large-scale image for 0.11 ML water adsorbed on a bitartrate island. (c) Details of (b) showing water forming mobile features and diffuse structures in the Cu channels between bitartrate rows. Increasing the water coverage to 0.25 ML (d) results in large amorphous clusters appearing along the Cu channels above low contrast zigzag structures. (e) Schematic showing the surface Cu net, indicated by the grid, and the location of bitartrate in (d) relative to the features caused by water in the Cu channels. The images were recorded at (a,b) −0.1 V, 10 pA, (c) −0.21 V, 20 pA, and (d) −0.21 V, 100 pA, respectively.

bitartrate rows as hydrophobic sites, despite the presence of OH groups on bitartrate that might stabilize water above the bitartrate chain.

Increasing the surface temperature increases the mobility of both water and bitartrate and changes the adsorption behavior, as shown in Figure 3. The zigzag water structures seen at 80 K (Figure 2d) disappear from the Cu channels, which implies these structures are metastable. Water surrounding the edge of bitartrate islands orders into recognizable H-bonding networks similar to those seen on clean Cu(110).[30,31] Apart from the appearance of large water clusters in the Cu channels as the coverage is increased (Figure 3g), STM no longer images any other water directly, but its presence can be inferred from changes to the bitartrate structure. We observe two distinct types of change to the bitartrate layer. The first, most common change observed at low temperature ($T \leq 120$ K) is an increase in contrast of bitartrate molecules along the edge of the trimer rows, to form a series of bright features down one or both sides of the bitartrate row, as shown in Figure 3a (see also Figure S1). The increase in contrast is associated with a slight shift (less than one-half the Cu spacing) in the intensity maximum of these features along the bitartrate row, as shown in Figure 3b. Formation of the bright rows maintains the overall bitartrate structure, with no increase in trimer width, and occurs occasionally even at 80 K.

The second type of modification to bitartrate is more significant and involves local restructuring of the trimer chains. At these sites, the outer bitartrate molecules increase in intensity, and some of the bitartrate groups change their adsorption footprint and site. An example is shown circled in Figure 3d, where a pair of bitartrate trimers increase in contrast and are displaced relative to the underlying Cu grid. The central molecule of the trimer changes appearance, aligning more along ⟨001⟩, and displaces by one-half a unit along ⟨1$\bar{1}$0⟩, consistent with bitartrate moving from an oblique footprint across two Cu unit cells to a rectangular adsorption site in a single Cu unit cell, as illustrated in Figure 3e,f. Simultaneously, the outer molecule displaces in the same direction and increases in contrast. This results in an increased width for the trimer chain, with bitartrate sitting in the adsorption sites expected for a $R_{ec}R_{ec}R_{ec}$ trimer, creating bare Cu sites within the structure that are not bonded to bitartrate (highlighted in yellow in Figure 3f). This rearrangement often occurs to several bitartrate trimers in a local group, which suggests the process is concerted, with bitartrate rearrangement creating space within the chains that allows water into the structure and encourages further disruption of neighboring sites. As the water dose is increased, Figure 3g, large water clusters form along the Cu channels and obscure many of the outer bitartrate groups. Nevertheless, the bitartrate along the center of the original trimer chains remains clear of water clusters, with individual molecules displaced irregularly on either side of the original site, similar to bitartrate in Figure 3d. Heating the surface to 150 K or above (Figure 3h) desorbs water that is stabilized only by weak water–water H-bonds[32] and removes the water clusters seen at lower temperature to leave only strongly bonded water. The increased mobility of water and bitartrate at 150 K results in the complete disappearance of the original bitartrate chains. The surface now consists of bitartrate adsorbed across the surface in a disordered fashion, Figure 3h, and the original bitartrate structure can only be recovered by annealing the surface to the original preparation temperature (350–400 K) to drive off the remaining water and reorder bitartrate. The progression from local changes to the bitartrate chains at low temperature (80 K) to complete dissolution at higher temperature (150 K) indicates that water progressively disrupts the tartaric acid structure and solvates the bitartrate units to form a disordered, hydrated 2D bitartrate–water phase.

To understand the mechanism by which bitartrate is solvated, we performed extensive DFT calculations to explore how water binds, what causes some molecules at the outside of the trimer chains to increase in contrast, and why water breaks apart the bitartrate structure. A summary of the calculated structures, their binding energy, and STM simulations is provided in the Supporting Information. The calculations show that water prefers to bind flat atop Cu to form a hydrogen bond to the O ligand of bitartrate, as shown in Figure 4a. The adsorption geometry is similar to that of water on the bare surface, but the binding energy for water is 0.466 eV greater than that for an isolated water on Cu and 0.195 eV greater than that for the pentamer chains formed on bare Cu terraces.[29] The four Cu sites immediately adjacent to the O

https://dx.doi.org/10.1021/jacs.0c04747
J. Am. Chem. Soc. 2020, 142, 13814–13822

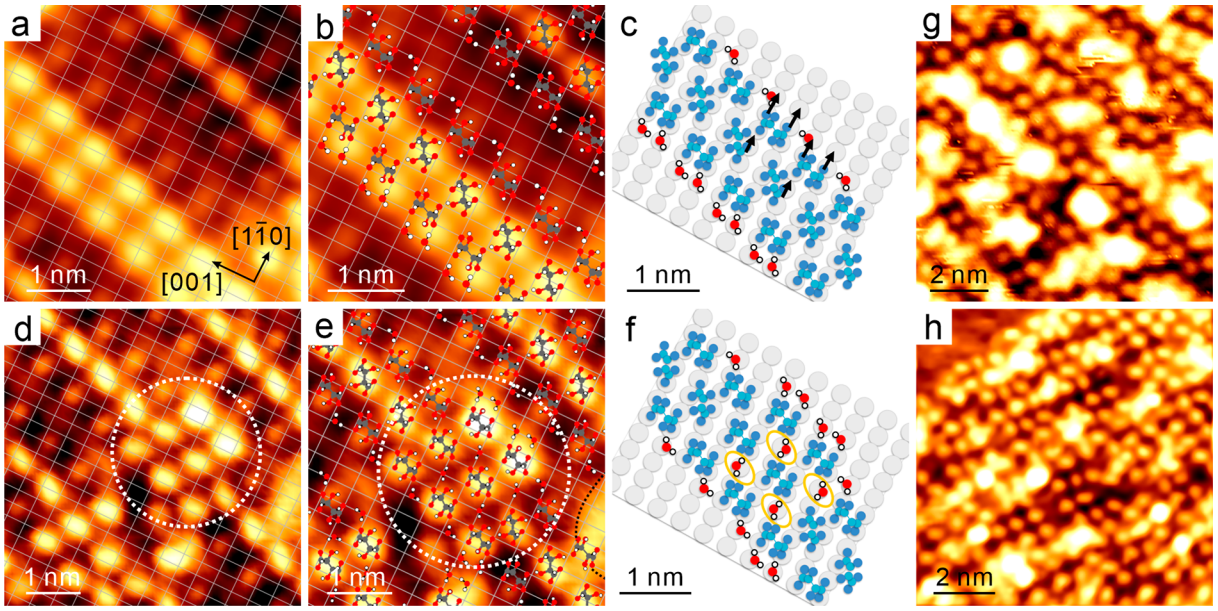

Figure 3. STM images showing the effect of water on bitartrate as the temperature is increased. (a,d) STM images showing details of the bitartrate structure in the presence of 0.1 ML water at 120 K. The grid shows the underlying Cu surface net. Part (a) shows a row of bitartrate along the edge of a trimer row increasing in contrast, while part (d) shows water locally expanding the trimer row and disrupting the original bitartrate structure (circled). Parts (b,c) and (e,f) show schematics, based on DFT calculations described in the text, which indicate water−bitartrate arrangements consistent with images (a) and (d). The solid arrows in (c) show the movement required to change the two bitartrate trimers (c) into the structure shown in (d)−(f). In (g), increasing the water coverage (ca. 0.5 ML) at 120 K forms water clusters in the Cu channels, while (h) shows the complete loss of long-range order of bitartrate after the surface is annealed to 150 K to remove weakly bound water clusters. The imaging conditions are (a,d,h) 0.4 V, 100 pA and (g) 0.34 V, 100 pA.

ligands all offer a similar binding energy, but when water donates to the O ligand adjacent to the OH group, the internal H-bond breaks and re-forms to the opposite carboxylate ligand, which distorts the bitartrate structure. The presence of two H donors alongside the bitartrate causes the internal H-bond to break entirely, as shown in Figures 4b and S6, which leaves the OH group pointing away from the surface. Despite breaking the internal bitartrate hydrogen bond, water adsorption has a negligible effect on the relative stability of the R_{ec} versus O_b footprints (see Figures S4−S6).

Water adsorption onto the extended bitartrate structure follows a similar pattern, with water preferentially decorating the edge of the trimer rows as it forms a hydrogen bond to the O ligands (Figure S7). Figure 4c shows the most stable structure we found with water decorating one edge of the trimer row. Water binds between two bitartrate molecules, to form a hydrogen bond to an O ligand on each molecule. Formation of the new water H-bond causes bitartrate to reorient its internal H-bond so the OH group binds to the opposite O ligand in a six-member ring. Water shows a low contrast in STM, and simulations (Figures 4c) show that the water molecules are invisible next to bitartrate and cannot be directly imaged in STM. When additional water is adsorbed onto this structure, it binds flat in the Cu channel, to form H-bond networks that show a low contrast in STM (see Figure S8 and the Supporting Information for more details). These structures are metastable, less stable than structures where water and bitartrate are allowed to fully restructure, but will form kinetically at low temperature as water decorates the stable hydration structure. This behavior reproduces the experimental observation that a low contrast water network forms in the Cu channel at 80 K (Figure 2d) but disappears when the surface is annealed to 120 K (Figure 3a,d), and water and bitartrate are able to relax into more stable configurations.

When a second water is added alongside bitartrate, water forms a dimer next to the O ligands, as shown in Figures 4d and S7. In this case, the water H-bonds to the O ligands cause bitartrate to completely break the internal hydrogen bond, so that the OH group now becomes free to rotate. STM simulations (Figure 4d) show a large increase in contrast to the bitartrate near the free OH, consistent with the shift in intensity maximum toward that end of the molecule observed experimentally (Figure 3b). Decoration of the edge of the bitartrate chains requires no displacement of the adsorbate and only limited local relaxation of the structure as water bonds to the O ligands and breaks the internal hydrogen bond. As a result, this process is expected to have a low activation barrier and is observed occasionally even at 80 K, but occurs more frequently above 100 K (Figure S1). Experimentally, we find that the contrast increase in bitartrate often occurs for a number of neighboring molecules, as shown in Figure 3a, which suggests an ordered chain of water forms alongside the bitartrate row, to cause the same relaxation at a series of sites. The DFT calculations support the idea that the local coordination around bitartrate determines if the internal OH group simply relaxes (Figure 4c) or breaks (Figure 4d), which causes the bitartrate to "light up" in STM. These results indicate that hydration of the O ligands along the edge of the Cu channels occurs even at 80 K and represent the first stage of bitartrate hydration.

To understand why water causes expansion of the bitartrate structure at higher temperatures (Figure 3d,h), we compared water adsorption on the original bitartrate arrangement with structures obtained by displacing bitartrate into a different site or footprint. Water adsorption on top of the original ($R_{ec}O_bR_{ec}$)

https://dx.doi.org/10.1021/jacs.0c04747
J. Am. Chem. Soc. 2020, 142, 13814−13822

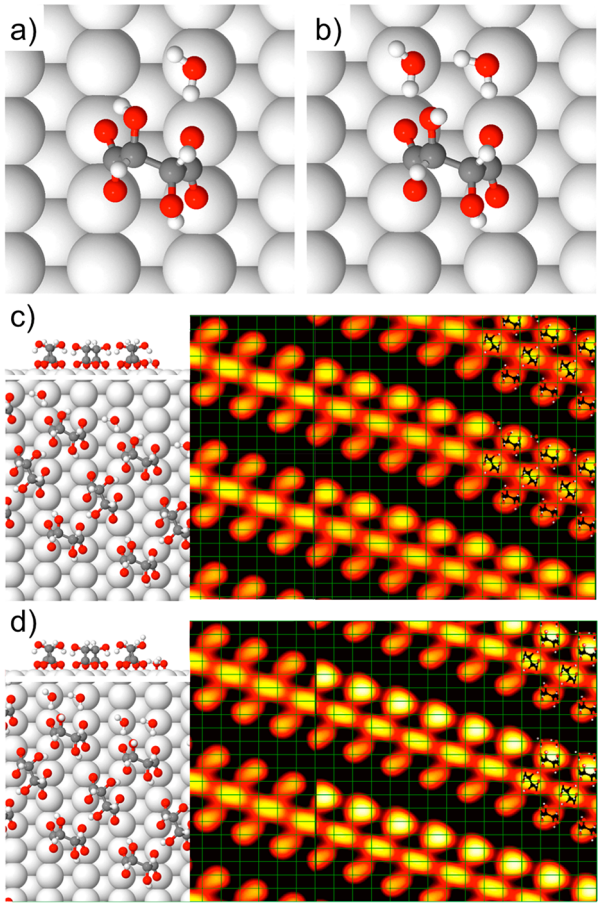

Figure 4. Electronic structure calculations showing the minimum energy adsorption geometry of one or two water molecules next to bitartrate, with a binding energy of (a−d) 0.957, 1.04, 1.089, and 1.04 eV/water, respectively. Parts (a,b) show water next to bitartrate monomer with the rectangular footprint, and parts (c,d) show the water structure next to bitartrate rows. The background in (c,d) compares a simulation of the STM images (0.3 V bias) showing bitartrate alone (LHS) or with water (RHS). The grid indicates the position of the Cu atoms. The contrast of bitartrate in (d) increases as 2 waters bind to the O ligands, which breaks the internal H-bond and shifts the maximum contrast toward the uncoordinated OH group (see Figure 3a−c).

bitartrate structure is extremely unfavorable, but restructuring the chains by changing the adsorption footprint, or by displacing bitartrate into neighboring sites, creates open chains with new adsorption sites that strongly bind water (Figure S9). Displacing bitartrate laterally creates the ($R_{ec}R_{ec}R_{ec}$) trimer observed in Figure 3d, which opens vacant Cu sites between the bitartrate groups, as shown schematically in Figure 3e,f. Water can adsorb at these vacant Cu sites as shown in Figure 5, hydrating the O ligands in the interior of the chains and stabilizing the ($R_{ec}R_{ec}R_{ec}$) configuration. This structure is the most stable arrangement we found with 2 waters per trimer and is more stable than structures where water decorates the edge of the bitartrate rows. Water adsorbs atop the vacant Cu site, to form H-bonds to the two neighboring O ligands. Although the new structure has sacrificed the intermolecular H-bond found in the original ($R_{ec}O_bR_{ec}$) trimer, this is compensated by the additional hydration energy. However, unlike relaxation of the internal H-bonds at the edge of a bitartrate row, restructuring a trimer requires the O ligands to

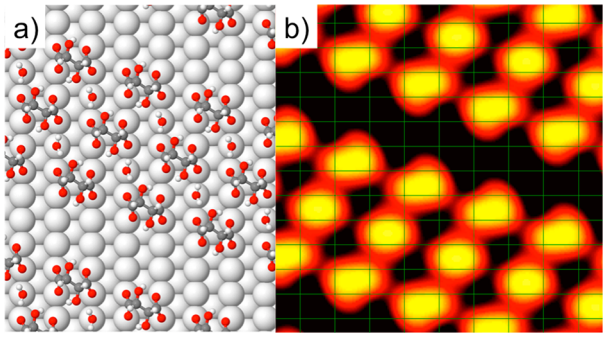

Figure 5. Calculated structure showing the most stable arrangement found for two water molecules adsorbed per bitartrate trimer with a binding energy of 1.235 eV/water. Part (a) shows the resulting $R_{ec}R_{ec}R_{ec}$ trimers with water adsorbed on the exposed Cu site. (b) Empty state STM simulation for 0.3 V bias with the grid showing the Cu surface net.

displace along the close-packed Cu row. This process is activated and occurs only occasionally at 80 K but becomes more common as the temperature is increased toward 120 K where there is sufficient thermal energy to allow bitartrate to change adsorption site. The formation of water H-bonds to the O ligands in the ($R_{ec}R_{ec}R_{ec}$) trimer causes the internal bitartrate H-bonds to reorient toward O on the opposite end of the molecule, which twists the C skeleton and increases the contrast in STM, Figure 5b, similar to the experimental behavior shown in Figure 3d. At higher temperatures, where mobility is greater, further restructuring can provide additional Cu adsorption sites, which allows more water into the rows and eventually causes the complete breakup of the bitartrate structure shown in Figure 3h. In support of this idea, several different trimer arrangements that allow water into the structure are more stable than structures with water confined to the outside edge alone (see Figure S9).

The idea that hydration of O ligands within the interior of the structure drives bitartrate restructuring gains further support from the observation of similar changes for isolated bitartrate trimers. In this case, it is possible to directly resolve the water network formed around the trimer; see Figures 6 and S3. Bitartrate trimers are immediately recognizable as three bright features, surrounded by a low contrast 2D water network in STM images. The water/OH hydrogen-bond structures can be assigned on the basis of previous work,[29−36] to define the Cu surface net and allow the trimer to be assigned to a particular configuration. Whereas $R_{ec}O_bR_{ec}$ trimers are found exclusively on the clean surface, and may persist up to ca. 120 K during hydration (see Figure S3), at higher temperatures hydration creates open $R_{ec}R_{ec}R_{ec}$ trimers, shown in Figure 6. Just as for the extended 2D structure, restructuring the trimer allows water greater access to the O ligands between the groups, with two new O ligands becoming accessible to water in the more open $R_{ec}R_{ec}R_{ec}$ structure (indicated by the dark blue O atoms shown schematically in Figure 6b).

Our results show that hydration of chemisorbed bitartrate is driven by the high binding energy of water at metal sites immediately next to carboxylate O ligands. The original bitartrate structure has accessible O−Cu ligands available along the edge of the bitartrate rows, and water decorates these sites at low temperature. Local relaxation of the internal bitartrate H-bonds occurs in response to the new water H-bonds, with multiple water H-bonds breaking the internal

https://dx.doi.org/10.1021/jacs.0c04747
J. Am. Chem. Soc. 2020, 142, 13814−13822

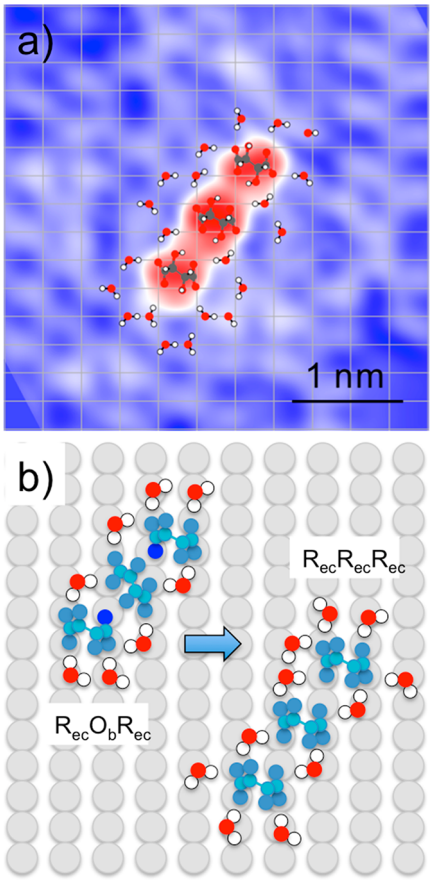

Figure 6. (a) STM image showing a single $R_{ec}R_{ec}R_{ec}$ trimer surrounded by a water/OH network after annealing at 150 K to order water (−0.4 V, 100 pA). The trimer images with a high contrast (red), while the water network appears as a low contrast (white) network above the Cu (blue), with the Cu lattice sites indicated by the grid. The occupied water adsorption sites immediately around the bitartrate trimer are indicated schematically, although the specific proton orientations are unknown. (b) Schematic comparing the number of water H-bonding sites around the original $R_{ec}O_bR_{ec}$ hydrogen-bonded trimer (left) to that of the relaxed $R_{ec}R_{ec}R_{ec}$ trimer (right). Oxygen ligand sites that are inaccessible to water in the original $R_{ec}O_bR_{ec}$ trimer are highlighted in bright blue, which show the creation of additional water adsorption sites around the $R_{ec}R_{ec}R_{ec}$ trimer.

bitartrate H-bond even at low temperature. In contrast, water adsorbed on top of the bitartrate structure, where it can form H-bonds to the OH group and O ligands, loses the favorable Cu−water interaction and is unstable. The original trimer rows do not have any vacant Cu sites within the structure where water could bind, but increasing the temperature allows water to penetrate into the rows and displace bitartrate to create stable Cu adsorption sites between the O ligands. Heating to 150 K causes the trimers to separate, which fully hydrates the O ligands and completely disrupts the original bitartrate structure, a process that occurs some 200 K below the temperature required to reorder bitartrate alone. By replacing the intermolecular H-bonds that stabilize bitartrate trimers with H-bonds to water, water adsorption destroys the long-range chiral structure. We conclude that any chiral activity of surface bitartrate in the presence of water can only arise from a direct local interaction with bitartrate.

Many supported adsorbate systems used in technical applications, such as surface protection or functionalization, rely on their wetting behavior to different materials for their operation,[37−39] which creates great interest in how water is structured within and immediately above the surface film.[13,40−42] Surface functionalization is often achieved by patterning the surface with an organic functional group, mediated by specific adsorption of the self-assembled layer via a polar ligand. Examples of such systems include SAMs based on S-, O-, or N-containing ligands, but experimental characterization of these overlayers remains limited.[43,44] Recently, new neutron reflection studies have revealed that Au thiol SAMs, probably the most intensively investigated system, show an unanticipated degree of water penetration into the interface, with between 2 and 6 waters per adsorbed ligand,[45] which directly influences the behavior of the SAM. The behavior displayed for the bitartrate system investigated here indicates that hydration of polar surface−adsorbate ligands is expected to occur by adsorption at nearest neighbor surface sites, which suggests a general mechanism for water adsorption on hydrophilic surfaces protected by an adsorbate film. A better understanding of the atomic arrangement of these interfaces will provide a way to anticipate the effect of this water and the consequences for surface packing and the growth or disruption of self-assembled films.

CONCLUSION

We have shown that hydration of a chiral, supramolecular assembly is driven by hydration of the O ligands that are responsible for binding the adsorbate to the metal surface. Initially the accessible O−Cu ligands are decorated by water, but, as the coverage increases, water disrupts the dense adsorbate chains and breaks the intermolecular H-bonds to allow water in to hydrate all of the O ligands. This process is progressive, with local restructuring allowing further water into the structure. Despite having an OH group that can form H-bonds to water, the bitartrate itself appears hydrophobic, with the OH groups playing a limited role in hydration. Because many supported adsorbate systems rely on highly polar ligands to chemisorb on the surface, we anticipate that hydration of polar surface−adsorbate ligands will play a key role in the hydration behavior of many technically important surfaces.

METHODS

Experimental Section. The Cu(110) surface was prepared by argon ion sputtering at 500 eV, followed by annealing to 800 K, to yield an average terrace size of ca. 800 Å. Further details have been given previously.[30] *R,R*-Tartaric acid (99%) was obtained from Sigma-Aldrich and used without purification. The adsorbate was deposited from a solid sample held in a resistively heated glass tube, separated from the main vacuum chamber by a gate valve and differentially pumped by a turbomolecular pump.[24] The tartaric acid was outgassed at ca. 340 K and then heated to ca. 370 K to sublime onto the copper crystal. After deposition, the Cu sample was heated to 350 K to deprotonate the acid and desorb the hydrogen. The ordering of the bitartrate phase and its structure was confirmed by LEED and STM.

STM images were recorded in an ultra high vacuum STM (Createc STM/AFM at 77 K) operated in constant current mode with an electrochemically etched tungsten tip. Images were acquired in constant current mode, with bias voltages quoted as the sample relative to the tip, so that positive voltages correspond to electrons tunneling into the surface (empty state images). Water was adsorbed on the bitartrate structures in situ at 80 K using a directional doser. The surface was then annealed to the desired temperature using a diode heater, before being cooled to 80 K to image the surface. Heating the surface from 80 to 150 K to desorb water clusters required ca. 2 h. STM images were processed using WSxM.[46]

https://dx.doi.org/10.1021/jacs.0c04747
J. Am. Chem. Soc. 2020, 142, 13814−13822

Preliminary experiments to characterize water adsorption in this system were carried out using a Specs 150 Aarhus STM at 100 K, with low current LEED and TPD to characterize water adsorption using methods described earlier.[47,48] Figures S1−S3 show supporting STM images of water adsorption on the 2D bitartrate structure and around an isolated trimer. Assignment of bitartrate to different adsorption footprints (R_{ec} or O_b) is made using the location of the bitartrate relative to the Cu surface net. The Cu atom locations are established either from the Cu location in STM (isolated trimers or small bitartrate islands), from the known structure of the bitartrate phase (large bitartrate islands at $T \leq 120$ K), or from the OH/water network around an isolated trimer (e.g., Figure 6). It is not possible to establish the bitartrate adsorption site and footprint when no ordered structure is present, for example, when bitartrate is fully hydrated and disordered at 150 K (Figure 4h).

Computational Details. Total energy calculations were carried out for trial structures using VASP[49,50] with the optB86b-vdW exchange-correlation functional.[51,52] The optB86b-vdW functional includes van der Waals interactions, which are known to be important in stabilizing surface adsorption relative to cluster formation,[53,54] and has a performance similar to that of other vdW functionals for systems where physisorption is important.[55] Water adsorption on a single bitartrate was modeled with a (5 × 4) supercell in a five-layer slab, with the bottom two layers fixed, using a 7 × 6 × 1 *k*-point mesh (see Figures S3−S5). The extended 2D structure in the (9 0,1 2) (*R*,*R*) unit cell used a 4 × 12 × 1 *k*-point set; see Figures S6−S8. Valence electron−core interactions were included using the projector augmented wave method,[56,57] with a plane wave cutoff energy of 400 eV and including dipole corrections perpendicular to the surface. All water adsorption energies are quoted in electronvolts per molecule, calculated relative to the original bitartrate covered Cu(110) surface and water in the gas phase. Adsorption energies are not corrected for vibrational effects. Figures S3−S8 show supporting calculations referred to in the text. Simulation of the STM images was calculated using the Tersoff−Hamann approximation in the implementation by Lorente and Persson.[58,59]

■ ASSOCIATED CONTENT

Supporting Information

The Supporting Information is available free of charge at https://pubs.acs.org/doi/10.1021/jacs.0c04747.

Additional STM images, electronic structure calculations, and binding energies for all of the structures discussed in the text (PDF)

■ AUTHOR INFORMATION

Corresponding Author

Andrew Hodgson − *Surface Science Research Centre and Department of Chemistry, University of Liverpool, Liverpool L69 3BX, United Kingdom;* orcid.org/0000-0001-8677-7467; Email: ahodgson@liverpool.ac.uk

Authors

Chenfang Lin − *Surface Science Research Centre and Department of Chemistry, University of Liverpool, Liverpool L69 3BX, United Kingdom;* orcid.org/0000-0001-5609-4358

George R. Darling − *Surface Science Research Centre and Department of Chemistry, University of Liverpool, Liverpool L69 3BX, United Kingdom*

Matthew Forster − *Surface Science Research Centre and Department of Chemistry, University of Liverpool, Liverpool L69 3BX, United Kingdom*

Fiona McBride − *Surface Science Research Centre and Department of Chemistry, University of Liverpool, Liverpool L69 3BX, United Kingdom*

Alan Massey − *Surface Science Research Centre and Department of Chemistry, University of Liverpool, Liverpool L69 3BX, United Kingdom*

Complete contact information is available at: https://pubs.acs.org/10.1021/jacs.0c04747

Notes

The authors declare no competing financial interest.

■ ACKNOWLEDGMENTS

This work was supported by the EPSRC via grant EP/K039687/1 and used the UK Materials and Molecular Modelling Hub for computational resources, via our membership of the UK's HEC Materials Chemistry Consortium funded by EPSRC (EP/L000202, EP/R029431), which is partially funded by EPSRC (EP/P020194). Work was also undertaken on Barkla, part of the High Performance Computing facilities at the University of Liverpool, UK.

■ REFERENCES

(1) Li, G. N.; Wang, B.; Resasco, D. E. Water-Mediated Heterogeneously Catalyzed Reactions. *ACS Catal.* **2020**, *10* (2), 1294−1309.

(2) Zhao, Z.; Bababrik, R.; Xue, W. H.; Li, Y. P.; Briggs, N. M.; Nguyen, D. T.; Nguyen, U.; Crossley, S. P.; Wang, S. W.; Wang, B.; Resasco, D. E. Solvent-mediated charge separation drives alternative hydrogenation path of furanics in liquid water. *Nature Catalysis* **2019**, *2* (5), 431−436.

(3) Bodenschatz, C. J.; Xie, T. J.; Zhang, X. H.; Getman, R. B. Insights into how the aqueous environment influences the kinetics and mechanisms of heterogeneously-catalyzed COH* and CH3OH* dehydrogenation reactions on Pt(111). *Phys. Chem. Chem. Phys.* **2019**, *21* (19), 9895−9904.

(4) Lucht, K.; Trosien, I.; Sander, W.; Morgenstern, K. Imaging the Solvation of a One-Dimensional Solid on the Molecular Scale. *Angew. Chem., Int. Ed.* **2018**, *57* (50), 16334−16338.

(5) Wu, C. H.; Pascal, T. A.; Baskin, A.; Wang, H.; Fang, H.-T.; Liu, Y.-S.; Lu, Y.-H.; Guo, J.; Prendergast, D.; Salmeron, M. B. The molecular scale structure of electrode-electrolyte interfaces: the case of platinum in aqueous sulfuric acid. *J. Am. Chem. Soc.* **2018**, *140* (47), 16237−16244.

(6) Li, C. Y.; Le, J. B.; Wang, Y. H.; Chen, S.; Yang, Z. L.; Li, J. F.; Cheng, J.; Tian, Z. Q. In situ probing electrified interfacial water structures at atomically flat surfaces. *Nat. Mater.* **2019**, *18* (7), 697.

(7) Cyran, J. D.; Donovan, M. A.; Vollmer, D.; Brigiano, F. S.; Pezzotti, S.; Galimberti, D. R.; Gaigeot, M. P.; Bonn, M.; Backus, E. H. G. Molecular hydrophobicity at a macroscopically hydrophilic surface. *Proc. Natl. Acad. Sci. U. S. A.* **2019**, *116* (5), 1520−1525.

(8) Mirabella, F.; Zaki, E.; Ivars-Barcelo, F.; Li, X. K.; Paier, J.; Sauer, J.; Shaikhutdinov, S.; Freund, H. J. Cooperative Formation of Long-Range Ordering in Water Ad-layers on Fe3O4(111) Surfaces. *Angew. Chem., Int. Ed.* **2018**, *57* (5), 1409−1413.

(9) Schaefer, J.; Backus, E. H. G.; Bonn, M. Evidence for autocatalytic mineral dissolution from surface-specific vibrational spectroscopy. *Nat. Commun.* **2018**, *9*, 3316.

(10) Esser, A.; Forbert, H.; Sebastiani, F.; Schwaab, G.; Havenith, M.; Marx, D. Hydrophilic Solvation Dominates the Terahertz Fingerprint of Amino Acids in Water. *J. Phys. Chem. B* **2018**, *122* (4), 1453−1459.

(11) Shavorskiy, A.; Aksoy, F.; Grass, M. E.; Liu, Z.; Bluhm, H.; Held, G. A Step toward the Wet Surface Chemistry of Glycine and Alanine on Cu{110}: Destabilization and Decomposition in the Presence of Near-Ambient Water Vapor. *J. Am. Chem. Soc.* **2011**, *133* (17), 6659.

(12) Saleheen, M.; Heyden, A. Liquid-Phase Modeling in Heterogeneous Catalysis. *ACS Catal.* **2018**, *8* (3), 2188−2194.

(13) Li, S. S.; Wu, L.; Zhang, X. F.; Jiang, X. E. The Structure of Water Bonded to Phosphate Groups at the Electrified Zwitterionic Phospholipid Membranes/Aqueous Interface. *Angew. Chem., Int. Ed.* **2020**, *59* (16), 6627−6630.
(14) Magnussen, O. M.; Gross, A. Toward an Atomic-Scale Understanding of Electrochemical Interface Structure and Dynamics. *J. Am. Chem. Soc.* **2019**, *141* (12), 4777−4790.
(15) Mallat, T.; Orglmeister, E.; Baiker, A. Asymmetric catalysis at chiral metal surfaces. *Chem. Rev.* **2007**, *107* (11), 4863−4890.
(16) Koshida, H.; Hatta, S.; Okuyama, H.; Shiotari, A.; Sugimoto, Y.; Aruga, T. Water-NO Complex Formation and Chain Growth on Cu(111). *J. Phys. Chem. C* **2018**, *122* (16), 8894−8900.
(17) Henzl, J.; Boom, K.; Morgenstern, K. Influence of water on supra-molecular assembly of 4,4 ‘-dihydroxy azobenzene on Ag(111). *J. Chem. Phys.* **2015**, *142* (10), 101920.
(18) Lechner, B. A. J.; Kim, Y.; Feibelman, P. J.; Henkelman, G.; Kang, H.; Salmeron, M. Solvation and Reaction of Ammonia in Molecularly Thin Water Films. *J. Phys. Chem. C* **2015**, *119* (40), 23052−23058.
(19) Lucht, K.; Loose, D.; Ruschmeier, M.; Strotkotter, V.; Dyker, G.; Morgenstern, K. Hydrophilicity and Microsolvation of an Organic Molecule Resolved on the Sub-molecular Level by Scanning Tunneling Microscopy. *Angew. Chem., Int. Ed.* **2018**, *57* (5), 1266−1270.
(20) Zhang, C.; Xie, L.; Ding, Y. Q.; Xu, W. Scission and stitching of adenine structures by water molecules. *Chem. Commun.* **2018**, *54* (7), 771−774.
(21) Tan, S. J.; Feng, H.; Zheng, Q. J.; Cui, X. F.; Zhao, J.; Luo, Y.; Yang, J. L.; Wang, B.; Hou, J. G. Interfacial Hydrogen-Bonding Dynamics in Surface-Facilitated Dehydrogenation of Water on TiO2(110). *J. Am. Chem. Soc.* **2020**, *142* (2), 826−834.
(22) Peng, J. B.; Guo, J.; Ma, R. Z.; Meng, X. Z.; Jiang, Y. Atomic-scale imaging of the dissolution of NaCl islands by water at low temperature. *J. Phys.: Condens. Matter* **2017**, *29* (10), 104001.
(23) Lorenzo, M. O.; Baddeley, C. J.; Muryn, C.; Raval, R. Extended surface chirality from supramolecular assemblies of adsorbed chiral molecules. *Nature* **2000**, *404* (6776), 376−379.
(24) Darling, G. R.; Forster, M.; Lin, C.; Liu, N.; Raval, R.; Hodgson, A. Chiral segregation driven by a dynamical response of the adsorption footprint to the local adsorption environment: bitartrate on Cu(110). *Phys. Chem. Chem. Phys.* **2017**, *19* (11), 7617−7623.
(25) Lawton, T. J.; Pushkarev, V.; Wei, D.; Lucci, F. R.; Sholl, D. S.; Gellman, A. J.; Sykes, E. C. H. Long Range Chiral Imprinting of Cu(110) by Tartaric Acid. *J. Phys. Chem. C* **2013**, *117* (43), 22290−22297.
(26) Hermse, C. G. M.; van Bavel, A. P.; Jansen, A. P. J.; Barbosa, L.; Sautet, P.; van Santen, R. A. Formation of chiral domains for tartaric acid on Cu(110): A combined DFT and kinetic Monte Carlo study. *J. Phys. Chem. B* **2004**, *108* (30), 11035−11043.
(27) Barbosa, L.; Sautet, P. Stability of chiral domains produced by adsorption of tartaric acid isomers on the Cu(110) surface: A periodic density functional theory study. *J. Am. Chem. Soc.* **2001**, *123* (27), 6639−6648.
(28) Lorenzo, M. O.; Haq, S.; Bertrams, T.; Murray, P.; Raval, R.; Baddeley, C. J. Creating chiral surfaces for enantioselective heterogeneous catalysis: R,R-Tartaric acid on Cu(110). *J. Phys. Chem. B* **1999**, *103* (48), 10661−10669.
(29) Carrasco, J.; Michaelides, A.; Forster, M.; Raval, R.; Hodgson, A. A Novel One Dimensional Ice Structure Built from Pentagons. *Nat. Mater.* **2009**, *8*, 427.
(30) Forster, M.; Raval, R.; Carrasco, J.; Michaelides, A.; Hodgson, A. Water-hydroxyl phases on an open metal surface: breaking the ice rules. *Chem. Sci.* **2012**, *3*, 93.
(31) Forster, M.; Raval, R.; Hodgson, A.; Carrasco, J.; Michaelides, A. c(2 × 2) water-hydroxyl layer on Cu(110): a wetting layer stabilized by Bjerrum defects. *Phys. Rev. Lett.* **2011**, *106*, 046103.
(32) Schiros, T.; Haq, S.; Ogasawara, H.; Takahashi, O.; Öström, H.; Andersson, K.; Pettersson, L. G. M.; Hodgson, A.; Nilsson, A. Structure of water adsorbed on the open Cu(110) surface: H-up, H-down, or both? *Chem. Phys. Lett.* **2006**, *429*, 415.
(33) Yamada, T.; Tamamori, S.; Okuyama, H.; Aruga, T. Anisotropic water chain growth on Cu(110) observed with scanning tunneling microscopy. *Phys. Rev. Lett.* **2006**, *96* (3), 036105.
(34) Kumagai, T.; Okuyama, H.; Hatta, S.; Aruga, T.; Hamada, I. Water clusters on Cu(110): Chain versus cyclic structures. *J. Chem. Phys.* **2011**, *134* (2), 024703.
(35) Shiotari, A.; Sugimoto, Y. Ultrahigh-resolution imaging of water networks by atomic force microscopy. *Nat. Commun.* **2017**, *8*, 14313.
(36) Hamada, I.; Kumagai, T.; Shiotari, A.; Okuyama, H.; Hatta, S.; Aruga, T. Nature of hydrogen bonding in hydroxyl groups on a metal surface. *Phys. Rev. B: Condens. Matter Mater. Phys.* **2012**, *86* (7), 075432.
(37) Zhang, J. L.; Gu, C. D.; Tu, J. P. Robust Slippery Coating with Superior Corrosion Resistance and Anti-Icing Performance for AZ31B Mg Alloy Protection. *ACS Appl. Mater. Interfaces* **2017**, *9* (12), 11247−11257.
(38) Wang, Z. X.; Elimelech, M.; Lin, S. H. Environmental Applications of Interfacial Materials with Special Wettability. *Environ. Sci. Technol.* **2016**, *50* (5), 2132−2150.
(39) Falde, E. J.; Yohe, S. T.; Colson, Y. L.; Grinstaff, M. W. Superhydrophobic materials for biomedical applications. *Biomaterials* **2016**, *104*, 87−103.
(40) Pawlowska, N. M.; Fritzsche, H.; Blaszykowski, C.; Sheikh, S.; Vezvaie, M.; Thompson, M. Probing the Hydration of Ultrathin Antifouling Organosilane Adlayers using Neutron Reflectometry. *Langmuir* **2014**, *30* (5), 1199−1203.
(41) Guo, P.; Tu, Y. S.; Yang, J. R.; Wang, C. L.; Sheng, N.; Fang, H. P. Water-COOH Composite Structure with Enhanced Hydrophobicity Formed by Water Molecules Embedded into Carboxyl-Terminated Self-Assembled Monolayers. *Phys. Rev. Lett.* **2015**, *115* (18), 186101.
(42) Fies, W. A.; First, J. T.; Dugger, J. W.; Doucet, M.; Browning, J. F.; Webb, L. J. Quantifying the Extent of Hydration of a Surface-Bound Peptide Using Neutron Reflectometry. *Langmuir* **2020**, *36* (2), 637−649.
(43) Liu, P. X.; Qin, R. X.; Fu, G.; Zheng, N. F. Surface Coordination Chemistry of Metal Nanomaterials. *J. Am. Chem. Soc.* **2017**, *139* (6), 2122−2131.
(44) Casalini, S.; Bortolotti, C. A.; Leonardi, F.; Biscarini, F. Self-assembled monolayers in organic electronics. *Chem. Soc. Rev.* **2017**, *46* (1), 40−71.
(45) Fies, W. A.; Dugger, J. W.; Dick, J. E.; Wilder, L. M.; Browning, K. L.; Doucet, M.; Browning, J. F.; Webb, L. J. Direct Measurement of Water Permeation in Submerged Alkyl Thiol Self-Assembled Monolayers on Gold Surfaces Revealed by Neutron Reflectometry. *Langmuir* **2019**, *35* (16), 5647−5662.
(46) Horcas, I.; Fernandez, R.; Gomez-Rodriguez, J. M.; Colchero, J.; Gomez-Herrero, J.; Baro, A. M. WSXM: A software for scanning probe microscopy and a tool for nanotechnology. *Rev. Sci. Instrum.* **2007**, *78* (1), 013705.
(47) McBride, F.; Hodgson, A. The reactivity of water and OH on Pt-Ni(111) films. *Phys. Chem. Chem. Phys.* **2018**, *20* (24), 16743−16748.
(48) Massey, A.; McBride, F.; Darling, G. R.; Nakamura, M.; Hodgson, A. The role of lattice parameter in water adsorption and wetting of a solid surface. *Phys. Chem. Chem. Phys.* **2014**, *16* (43), 24018−24025.
(49) Kresse, G.; Furthmuller, J. Efficient iterative schemes for ab initio total-energy calculations using a plane-wave basis set. *Phys. Rev. B: Condens. Matter Mater. Phys.* **1996**, *54* (16), 11169−11186.
(50) Kresse, G.; Hafner, J. Abinitio Molecular-Dynamics for Liquid-Metals. *Phys. Rev. B: Condens. Matter Mater. Phys.* **1993**, *47* (1), 558−561.
(51) Klimes, J.; Bowler, D. R.; Michaelides, A. Chemical accuracy for the van der Waals density functional. *J. Phys.: Condens. Matter* **2010**, *22* (2), 022201.

(52) Klimes, J.; Bowler, D. R.; Michaelides, A. Van der Waals density functionals applied to solids. *Phys. Rev. B: Condens. Matter Mater. Phys.* **2011**, *83* (19), 195131.
(53) Carrasco, J.; Santra, B.; Klimes, J.; Michaelides, A. To wet or not to wet? Dispersion forces tip the balance for water ice on metals. *Phys. Rev. Lett.* **2011**, *106*, 026101.
(54) Gillan, M. J.; Alfe, D.; Michaelides, A. Perspective: How good is DFT for water? *J. Chem. Phys.* **2016**, *144* (13), 130901.
(55) Hanke, F.; Dyer, M. S.; Bjork, J.; Persson, M. Structure and stability of weakly chemisorbed ethene adsorbed on low-index Cu surfaces: performance of density functionals with van der Waals interactions. *J. Phys.: Condens. Matter* **2012**, *24* (42), 424217.
(56) Blöchl, P. E. Projector augmented-wave method. *Phys. Rev. B: Condens. Matter Mater. Phys.* **1994**, *50*, 17953−17979.
(57) Kresse, G.; Joubert, D. From ultrasoft pseudopotentials to the projector augmented-wave method. *Phys. Rev. B: Condens. Matter Mater. Phys.* **1999**, *59*, 1758−1775.
(58) Tersoff, J.; Hamann, D. R. Theory And Application For The Scanning Tunneling Microscope. *Phys. Rev. Lett.* **1983**, *50* (25), 1998−2001.
(59) Lorente, N.; Persson, M. Theoretical aspects of tunneling-current-induced bond excitation and breaking at surfaces. *Faraday Discuss.* **2000**, *117*, 277−290.

https://dx.doi.org/10.1021/jacs.0c04747
J. Am. Chem. Soc. 2020, 142, 13814−13822